International Journal of ChemTech Research
CODEN (USA): IJCRGG, ISSN: 0974-4290, ISSN(Online):2455-9555
Vol.11 No.10, pp 41-51, 2018

Effect of Sodium Acetate Trihydrate Addition on Structural, Optical, Dielectric and NLO Properties of Thiourea Single Crystal

B. Neelakantaprasad[1]*, S. Masilamani[2] and B. Ravi[3]

[1]Department of Physics, K.S.R. College of Engineering, Tiruchengode – 637 215, Tamil Nadu, India.
[2]Department of Physics, K.S Rangasamy College of Technology, Namakkal – 637 215, Tamil Nadu, India.
[3]Department of Physics, Vidyaa Vikas College of Engineering and Technology, Tiruchengode – 637 214, Tamil Nadu, India.

Abstract : Optically fine quality single crystals of pure thiourea (abbreviated as TU) CH_4N_2S and sodium acetatetrihydrate doped thiourea (abbreviated as STATH) $NaC_3H_{13}N_2SO_5$ were effectively grown by slow evaporation method at room temperature from their aqueous solutions. The procured crystals were of average size 18×12×5 mm^3 (TU) and 17×8×5 mm^3 (STATH). Single and Powder X-ray Diffraction studies were consummated and the lattice specifications of the grown crystals have been assessed. Optical constants were appraised for both the samples by manipulating UV–Vis–NIR spectroscopy. Chemical composition of TU and STATH was scrutinized by EDX analysis. The dielectric response of both the samples was investigated in the frequency zone 100 Hz to 5 MHz besides solid state parameters were deliberated. The second harmonic generation (SHG) efficiency test manifests that STATH has the efficiency 1.506 times that of potassium dihydrogen phosphate (KDP).
Keywords : Crystal growth, Optical studies, EDX, Dielectric and NLO.

Introduction

Modern research is attentive on the search for deserved materials exposing excellent second order nonlinear optical (SONLO) properties for prospective applications in optoelectronics, telecommunication and optical storage devices. Materials with substantial second order optical nonlinearities, stubby transparency cut-off wavelengths and secure physicochemical performances are required to perceive many of these applications [1,2].TGDTA, microscopic, optical and spectral analyses are essential mechanisms for materials characterization. Some of the privileges of organic materials are flexibility in the mechanisms of synthesis, scope for amending the properties by functional substitution, inherently high nonlinearity and high damage resistance etc., A major disadvantage of crystalline organic materials is that they are difficult to be grown in

DOI= http://dx.doi.org/10.20902/IJCTR.2018.111007

bulk size, optical quality single crystals and also the vulnerable identity of these crystals makes them unfavourable for the technique in device significances. The inherent shortcomings on the maximum attainable nonlinearity in inorganic materials and the equitable prosperity in growing device grade organic single crystals have made scientists embrace auxiliary approaches. The conspicuous one was to thrive composite organic-inorganic materials having a few reciprocation in their appropriate rewards. This modern category of materials has come to be known as semi-organic [3-5] with metal-organic coordination compounds. Semi-organic materials procure significance over inorganic materials as a consequence of their immense polarizability, compendious transmission window and exorbitant damage threshold[6]. In modern years, endeavours have been made on amino acid with organic and inorganic complexes for prospective NLO applications [7].Recently elaborate inspection of metal complexes of thiourea analogs stated that they have superior nonlinear optical properties compared to those of standard potassium dihydrogen orthophosphate (KDP). The centrosymmetric thiourea molecules, when incorporated within organic salt furnish noncentrosymmetric complexes, which possess nonlinear optical properties[8]. The NLO properties of some complexes of thiourea have captivated consequential surveillance in the modern years, since both organic and inorganic elements in its ubscribe especially to the operation of SHG[9–11].Bisthiourea–ZincAcetate (BTZA)[12] and Cadmium thiourea acetate (CTA) are the precedents of these salt complexes [13]. In the current research, thiourea is incorporated with sodium acetate trihydrate to cultivate sodiumthiourea acetate trihydrate, an organometallic nonlinear optical(NLO)material. STATH crystallizes in the orthorhombic structure and the lattice specifications are delineated to be a= 7.6687Å,b= 8.5775Åand$c$= 5.44916Å.

2. Experimental

2.1. Synthesis and crystals growth

Alkali metal acetate (sodium acetate trihydrate) SATH was mixed with thiourea in a stoichiometric ratio of 1:1 in doubly distilled water and then stirred persistently for 6 hours for amalgamation. The chemical reaction is as follows

$CH_4N_2S + C_2H_9NaO_5 \rightarrow NaC_3H_{13}N_2SO_5$

Moreover, pure thiourea was dissolved in doubly distilled water and then stirred persistently for 6 hours for amalgamation. The purity of the product was procured by the action of replicated recrystallization. The complete dissolved solutions were percolated, manipulating micro filter paper and taken in two different beakers. They were optimally closed by manipulating a pricked polythene paper and kept in undisturbed conditions and the solution was permitted to evaporate slowly at room temperature. After a growth period of 30 days optically transparent TU single crystals of dimension 18×12×5 mm^3 were harvested while optically transparent and well developed STATH single crystals of dimension 17×8×5 mm^3 were harvested after 40 days. The photographs of grown single crystals are presented in **Fig-1 (a) & (b)**.

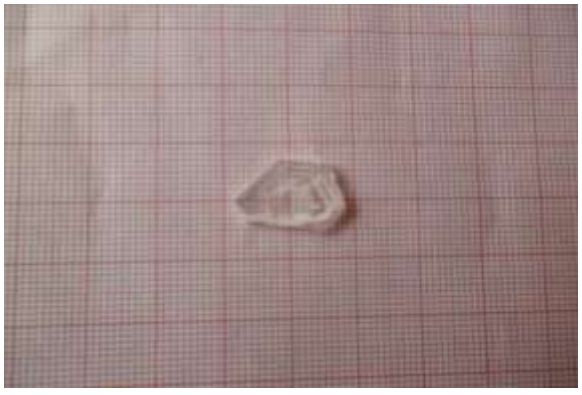

Fig 1(a) Photograph of TU

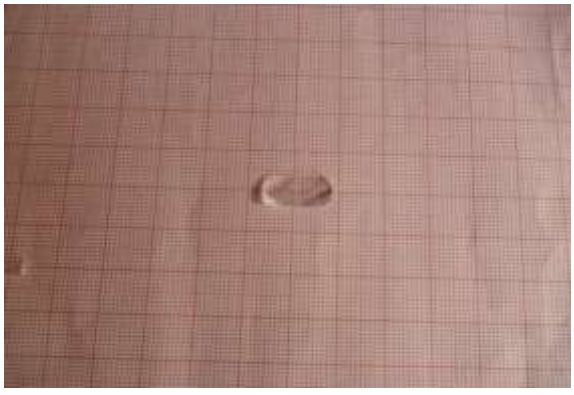

Fig 1(b) Photograph of STATH

2.2 Characterization Studies

In spite of affirm the crystalline nature and to ascertain the lattice specifications of the grown crystals TU and STATH, single crystal X-ray diffraction studies have been executed, employing Bruker axs kappa apex2 CCD Diffractometer with MoKα radiation in the wavelength 0.71073Å. Moreover, powder X-ray diffraction pattern of both the crystals were registered, employing Bruker Kappa Apex II diffractometer with CuKα radiation(λ = 1.5418 Å), at room temperature with a scanning speed of 1°/ min and a scanning range of 20 degrees to 80 degrees. UV–Vis–NIR spectroscopy is manipulated to assess the optical constants for both the samples. In order to procure the particulars about the chemical composition, the grown crystals were subjected to EDX analysis, employing the instrument Field emission scanning electron microscope JEOL-JSM- 6701 F (Japan) energy dispersive X-ray micro analyzer. The dielectric measurements of the grown crystals were executed manipulating HIOKI 3532-50 LCRHITESTER. The Second harmonic generation efficiency of both the crystals was computed using Kurtz and Perry powder technique.

3. Result and discussion

3.1 X-ray Diffraction Analysis

In favour of affirm the crystalline nature and to establish the lattice specifications of the grown crystals TU and STATH, single crystal X-ray diffraction studies have been executed employing Bruker axs kappa apex2 CCD Diffractometer with MoKα radiation in the wavelength 0.71073Å. The intended lattice specification values of TU are a= 7.5421 Å, b= 8.4213 Å, c= 5.3654 Å and **α=** β= γ= 90º and that of STATH are a= 7.6687 Å, b= 8.5775 Å, c= 5.4916 Å and **α=** β= γ= 90º**.** From these results, it is conspicuous that the lattice specification values of TU are slightly elevated by the incorporation of SATH and alsoit is comprehensible that both the crystals belong to the orthorhombic system. Furthermore, powder X-ray diffraction pattern of both the crystals were registered employing Bruker Kappa Apex II diffractometer with CuKα radiation(λ = 1.5418 Å) at room temperature with a scanning speed of 1°/ min and a scanning range of 20 degree to 80 degree. The powder X-ray diffraction pattern of TU and STATH are manifested in **Fig-2.** Perceivable Bragg peaks procured at specific 2θ angles stipulating that both the crystals are ordered.

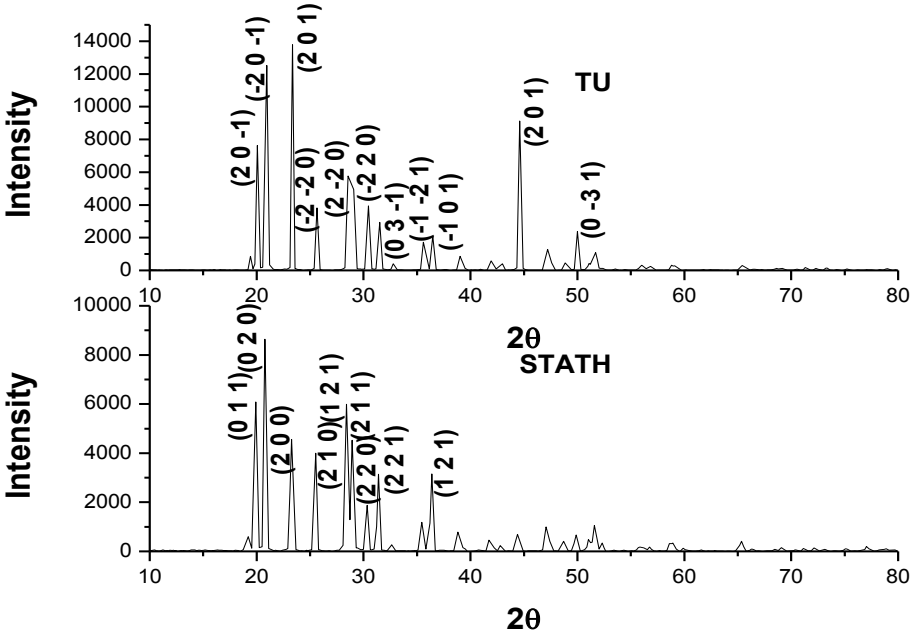

Fig- 2: Powder XRD Spectra of TU and STATH

The crystalline size (D) was deliberated for both the materials manipulating Scherrer's formula from the full width half maximum (β).

$$D = \frac{0.945\times\lambda}{\beta\ cos\theta} \quad (1)$$

The crystalline size of the cultivated crystals was established to be 88 nm (TU) and 79 nm (STATH). Moreover, it is noticeable that the crystalline size of TU decreased by the inclusion of SATH.

3.2 Optical studies

The UV–Vis–NIR absorption spectrophotometer was manipulated to register the transmission spectrum in the range between 200 nm and 1100 nm. Near IR spectroscopy is a valuable mechanism for scrutinizing aromatic mixtures. This sector discovers wide embrace in food and grain industry for the establishment of protein, fat, moisture, sugar, etc. Absorption computations in the UV and visible sectors furnish details about electronic transitions in a sample. The manipulation of a material in optoelectronic devices is decided by its optical etiquette. Optical transparency, absorption coefficient, band gap, extinction coefficient and the refractive index are the principal specifications to ascertain the optical properties of a crystal. The optical properties of the crystals are regulated by the interaction between the crystal and the electric and magnetic fields of the electromagnetic wave. The UV-Vis-NIR Spectrum of TU and STATH Crystals are manifested in **Fig- 3**. From the perceived spectrum, the lower cut-off wavelengths of STATH and TU were established to be 221 nm and 281 nm respectively. Moreover, the transmittance of TU was elevated because of the inclusion of SATH.

The estimated transmittance (T) was manipulated to enumerate the absorption coefficient (α), manipulating the relation,

$$\alpha = \frac{2.3026\ \log(1/T)}{t} \quad (2)$$

where T is the transmittance and t is the thickness of the crystal.

The optical band gap (Eg) was evaluated from the absorption spectrum and optical absorption coefficient (α) near the absorption edge, which is given by,

$$\alpha h\nu = A\sqrt{h\nu - E_g} \quad (3)$$

where Eg is the optical band gap of the crystal and A is a constant.

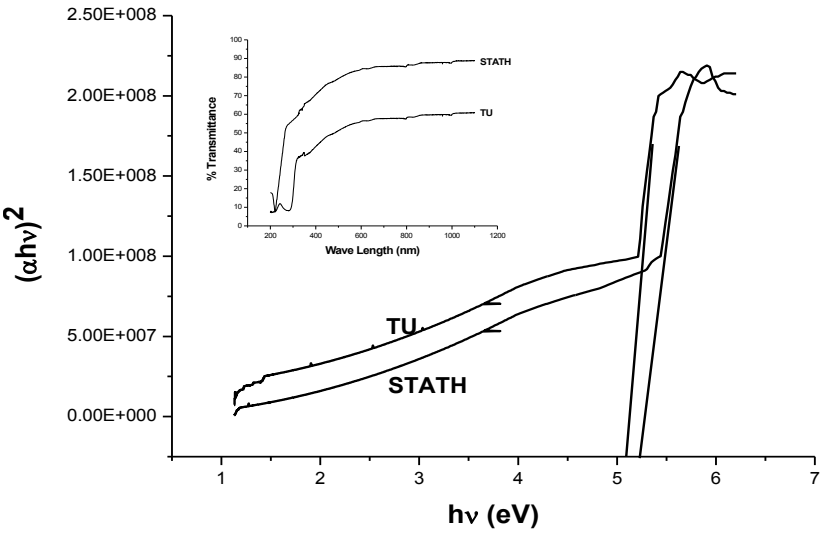

Fig-3: UV-Vis-NIR Spectrum and Band gap of TU and STATH Crystals

The Tauc's plot of $(\alpha h\nu)^2$ against the photon energy ($h\nu$) at room temperature (**Fig-3**) manifests a linear behaviour, (α- absorption coefficient and h-Planck's constant) which can be contemplated as an

authentication of the indirect transition. Hence, inferring the indirect transition between valence band and conduction band, the band gap (Eg) is estimated by the extrapolation of the linear portion of the curve to the point $(\alpha h\nu)^2$- 0. Exploiting this method, the band gap of TU crystal was established to be 5.109 eV and that of STATH was 5.22 eV. As a prominence of wide band gap, the grown crystals have a large transmittance in the visible region.

The extinction coefficient is the fragment of misplacement of light or electromagnetic energy because of scattering and absorption per unit thickness or distance in a specific medium. The extinction coefficient can also be described in electromagnetic terms as deteriorate or frustrate of the amplitude of the incident electric and magnetic fields. The variation of extinction coefficient (K) with wavelength for TU and STATH is manifested in **Fig-4 (a)**.From the graph, it is recognizable that the extinction coefficient (K) increases with increase in wavelength and also the K value of TU was increased by the insertion of SATH.

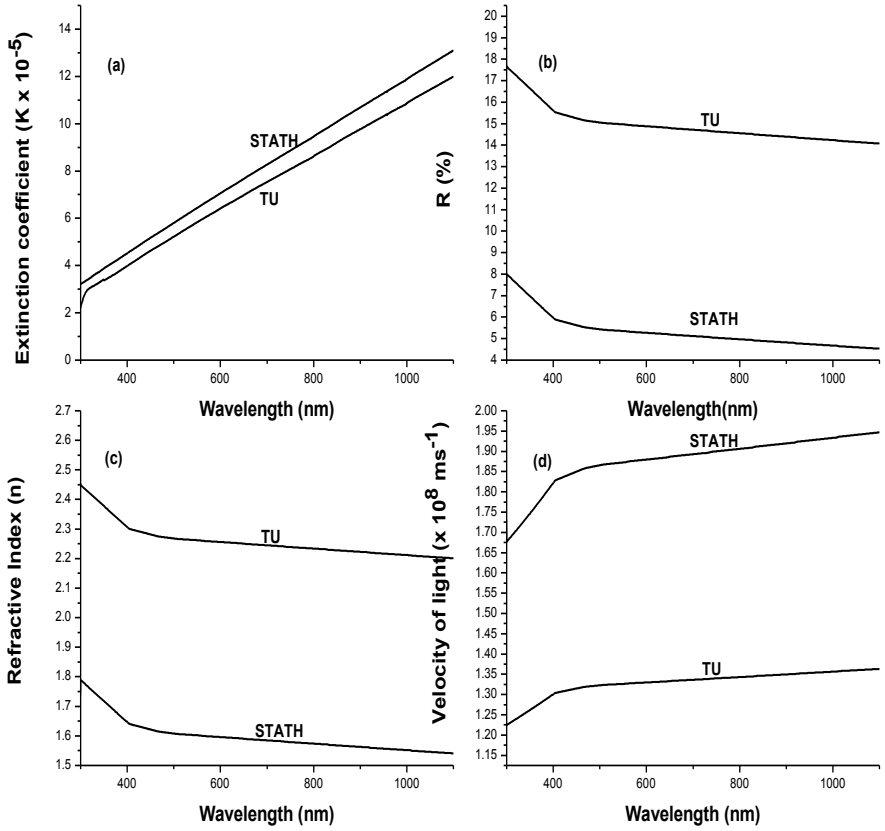

Fig-4: (a) Variation of K with Wavelength (b) Variation of R with Wavelength (c) Variation of n with Wavelength (d) Variation of c_m with Wavelength

The extinction coefficient (K) can be procured from the following equation

$$K = \frac{\lambda\alpha}{4\pi} (4)$$

The variation of extinction coefficient (K) with photon energy $(h\nu)$ for both the crystals is manifested in **Fig-5 (a)**. From the plot, it is observable that the value of K decreases with hν for both the materials. The low value of K displays the weak interaction between the photons and electrons in both the materials.

The transmittance (T) is given by

$$T = \frac{(1-R)^2 e^{-\propto t}}{1-R^2 e^{-2\propto t}} \quad (5)$$

Reflectance (R) in terms of the absorption coefficient can be procured from the above equation. Hence,

$$R = 1 \pm \frac{\left[1-e^{-\propto t}+e^{\propto t}\right]^{1/2}}{1-e^{-\propto t}} \quad (6)$$

The variation of Reflectance (R) with wavelength for both the samples is manifested in **Fig-4(b)**.

One more important property called refractive index (n) was scrutinized for both the crystals and it is a measure of the speed of light in the substance. It is elucidated as the ratio of the speed of light in vacuum to that in the considered medium.

The refractive index (n) can be ascertained from the reflectance data, employing the following equation

$$n = -(R+1) \pm 2\,\frac{(R)^{1/2}}{(R-1)} \quad (7)$$

The refractive index (n) of TU is 2.22 and that of STATH is 1.56 at λ = 900 nm. The variation of refractiveindex (n) with wavelength of the cultivated crystals is manifested in **Fig-4(c)**. From the plot, it is conspicuous that the refractive index of TU decreased because of the supplement of SATH.

The velocity of light in crystal (c_m) can be estimated for both the cultivated samples in terms of refractive index (n) manipulating the following relation:

$$c_m = \frac{c_a}{n} \quad (8)$$

where c_a is the velocity of light in air or vacuum. The variation of velocity of light (c_m) with wavelength for the grown samples is manifested in **Fig-4(d)** and it is obvious that the velocity of light increases with the increase in wavelength.

3.2.1 Electric susceptibility

From the optical constants n and K, electric susceptibility (χ_e) as a consequence of interband transition of free carriers can be computed for both the crystals on the basis of equation (9):

$$\varepsilon_0 + 4\pi\chi_e = n^2 - K^2 \quad (9)$$

Hence,

$$\chi_e = \frac{n^2-K^2-\varepsilon_0}{4\pi} \quad (10)$$

where ε_0 is the dielectric constant in the deprivation of any contribution from free carriers. The variation of electric susceptibility with photon energy of the cultivated samples is manifested in **Fig-5 (b)**. From the plot, it is evident that there is an increase in χ_e with hν for TU and STATH. Moreover, the electric susceptibility of TU was decreased because of the inclusion of SATH. The value of electric susceptibility χ_e is established to be 0.393 (TU) and 0.194 (STATH) at λ = 900 nm.

3.2.2 Optical and electrical conductivity

Optical conductivity (σ_{op}) is one of the specifications for studying the electronic states in materials. If a system is subjected to an external electric field then, in general, a redistribution of charges arises and hence currents are persuaded in the system. The persuaded polarization and the persuaded currents are proportional to the persuading field for small enough fields. The optical conductivity (σ_{op}) is a measure of the frequency reciprocation of the material when irradiated with light. The optical conductivity of the grown crystals was calculated, exploiting the following relation:

$$\sigma_{op} = \frac{\alpha n c}{4\pi} \quad (11)$$

where c is the velocity of light, α is the absorption coefficient and n is the refractive index. **Fig- 5 (c)** manifests the variation of the optical conductivity as a function of photon energy for TU and STATH crystals. From the graph, it is perceived that the optical conductivity directly pivots on absorption coefficient and the refractive index of the material and also for substantial energy values, an exponential increase was perceived in the optical conductivity of both the samples. This can be described in terms of the transfer of a large number of charge carriers from the valence to conduction band in TU and STATH crystals. TU and STATH crystals manifest high magnitude of optical conductivity (10^{10} s−1) and this affirms the existence of high photo reciprocation of the material and this property makes the material more illustrious for device applications in data processing and quantifying.

The electrical conductivity (σ_e) was enumerated for both the samples in terms of optical conductivity and absorption coefficient, by exploiting the following expression(12):

$$\sigma_{e} = \frac{2\lambda}{\alpha}\sigma_{op} \qquad (12)$$

where λ is the wavelength of light.

Low value of the electrical conductivity manifests the dielectric nature of the materials.The variation of electrical conductivity with photon energy of both the cultivated crystals is depicted in **Fig-5 (d)** and from the plot, it is evident that the electrical conductivity decreases with photon energy for both the crystals. Moreover, the optical and electrical conductivities of TU were decreased by the supplement of SATH

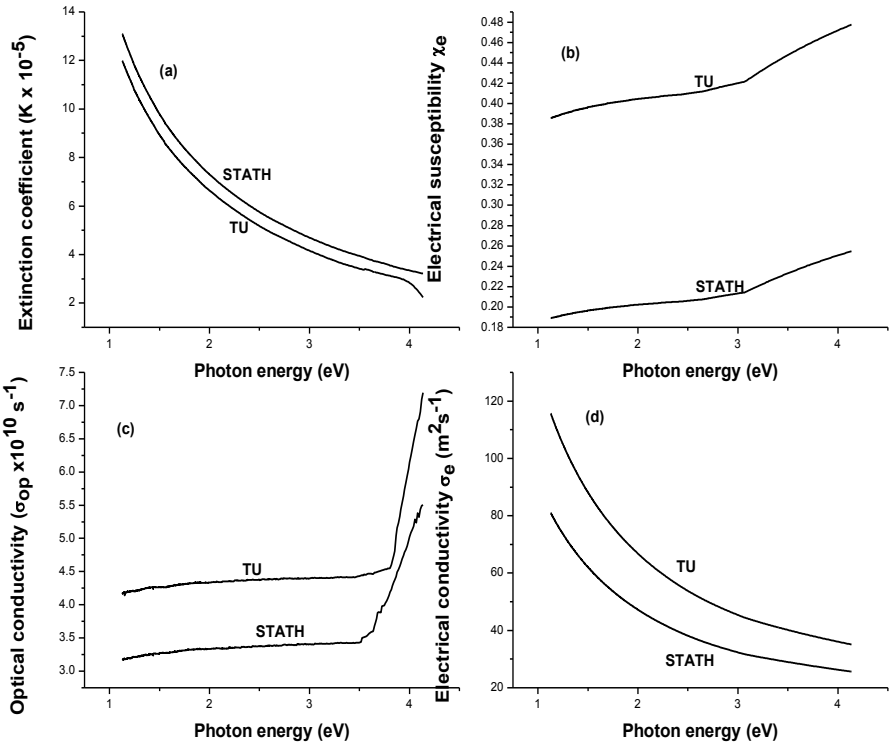

Fig-5: (a) Variation of K with $h\nu$ (b) Variation of χ_e with $h\nu$ (c) Variation of σ_{op} with$h\nu$ (d) Variation of σ_e with $h\nu$

3.3 EDX Analysis

In spite of procuring the details about the chemical configuration of the grown crystals, a meticulous technique called Energy-dispersive X-ray spectroscopy is manipulated. In this study, the grown crystals were subjected to EDX analysis manipulating the device Field emission scanning electron microscope JEOL-JSM-6701 F(Japan) energy dispersive X-ray micro analyzer. **Fig-6 (a) & (b)** manifest the counts per second versus

energy of EDX spectrum for TU and STATH crystals respectively. The peaks that correlate with Carbon, Nitrogen and Sulphur were observed for TU single crystal whereas the peaks that correlate with Carbon, Nitrogen, Sulphur, Sodium and Oxygen were observed for STATH single crystal. From the EDX spectrum the evolution of new crystal STATH was confirmed.

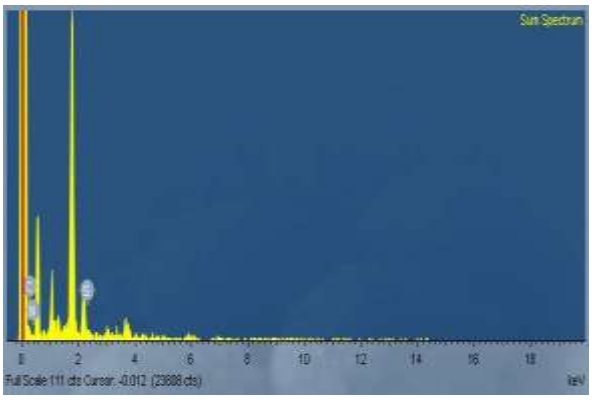

Fig-6(a): EDX spectrum of TU

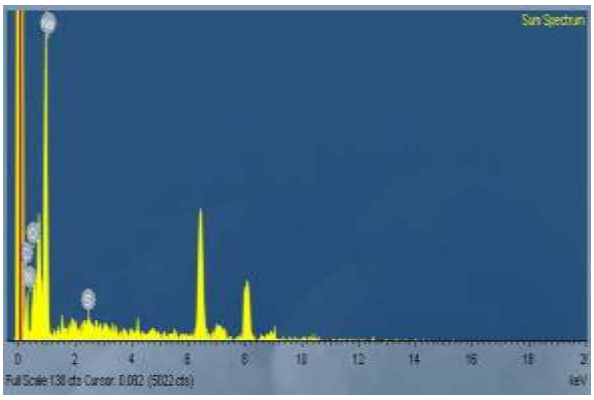

Fig-6(b): EDX spectrum of STATH

3.4 Dielectric Studies

The properties dielectric constant and the dielectric loss of TU and STATH were investigated at disparate temperatures, manipulating the HIOKI3532 LCR HITESTER in the frequency zone 100 Hz to 5 MHz. The dielectric constant and dielectric loss for TU and STATH were computed manipulating Agilent 4284-A LCR meter. The dimensions of the samples manipulated were 5x4x3 mm^3 (TU) and 6x5x4 mm^3 (STATH). Two conflicting surfaces across the breadth of the sample were treated with good quality silver pastes in spite of procuring fine ohmic contact. The dielectric constant was computed as a consequence of the frequency for the crystals TU and STATH at three disparate temperatures (40, 50 and 60° C) and is depicted in **Fig-7 (a) & (c)**, while the corresponding dielectric loss is depicted in **Fig-7 (b) & (d)** respectively. The dielectric constant was enumerated applying the relation,

$$\varepsilon_r = \frac{Cd}{\varepsilon_0 A} \qquad (13)$$

where d is the thickness of the samples and A is the area of the samples. It is perceived from **Fig-7 (a) & (c)** that the dielectric constant decreases exponentially with increasing frequency, and then procures almost a persistent value in the high frequency zone for both the samples. Moreover, this stipulates that the value of the dielectric constant increases with an increase in the temperature. The total polarization present in the material isowing to ionic, electronic, dipolar and space charge polarizations. The contribution to the decrease in the dielectric constant due to electronic polarization is absolutely less. **Fig-7 (b) & (d)** demonstrate that the dielectric loss is heavily dependent on the frequency of the applied field, similar to that of the dielectric constant.

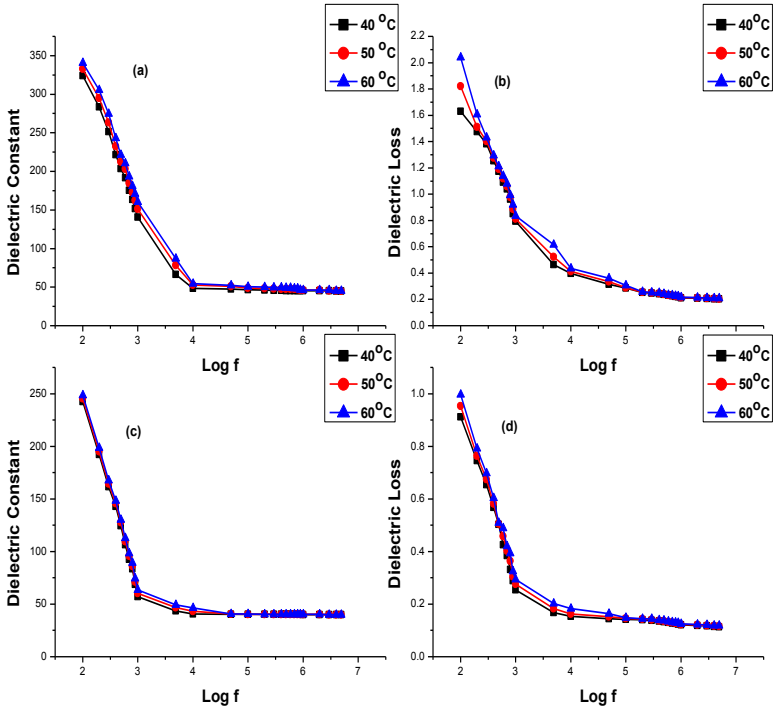

Fig-7 (a) Dielectric constant versus frequency of STATH (b) Dielectric Loss versus frequency of STATH (c) Dielectric constant versus frequency of TU (d) Dielectric Loss versus frequency of TU

The dielectric loss decreases with an increase in the frequency at nearly all temperatures, but appears to attain saturation in the higher frequency and above, at all the temperatures. In the low frequency region, prominent energy loss is perceived, which may be owing to the dielectric polarization, space-charge and rotation-direction polarization arising in the low frequency range. The prominent dielectric constant at low frequencies may be due to the existence of all the four polarizations, namely, space charge, orientation, electronic and ionic polarization and its low value at higher frequencies may be due to the gradual loss of consequence of these polarizations.

In the suggested relation, only one specification viz., the prominent frequency dielectric constant is required as the input for both the crystals to enumerate the electronic properties like valence electron plasma energy, average energy gap or Penn gap, Fermi energy and electronic polarizability. The theoretical calculations manifest that the high frequency dielectric constant is obviously dependent on the valence electron Plasmon energy, an average energy gap referred to as the Penn gap and Fermi energy. The Penn gap is determined by fitting the dielectric constant with the Plasmon energy.

$$\hbar\omega_p = 28.8\sqrt{\frac{Z\rho}{M}} \qquad (14)$$

$$Ep = \frac{\hbar\omega_p}{\sqrt{(\epsilon_\infty - 1)}} \qquad (15)$$

$$E_F = 0.2948\left(\sqrt[3]{(\hbar\omega_p)^4}\right) \qquad (16)$$

$$\propto = \left[\frac{(\hbar\omega_p)^2 S_0}{(\hbar\omega_p)^2 S_0 + 3Ep^2}\right] + \frac{M}{\rho} \text{ x } 0.396 \text{ x } 10^{-24} \text{ cm}^3 \qquad (17)$$

where S_0 is a constant given by

$$S_0 = 1 - \left[\frac{Ep}{4E_F}\right] + \frac{1}{3}\left[\frac{Ep}{4E_F}\right]^2 \qquad (18)$$

The value of ∝ procureed from Eq. (17) meticulously facsimiles with that procured, manipulating the Clausius–Mossotti relation,

$$\propto = \frac{3M}{4\pi N\rho}\left[\frac{\varepsilon_\infty - 1}{\varepsilon_\infty + 2}\right] \qquad (19)$$

Considering that the polarizability is prominently delicate to the bandgap (18), the following empirical relation Is also employed to enumerate ∝

$$\propto = \left[1 - \frac{(E_g)^{1/2}}{4.06}\right] \text{x } \frac{M}{\rho} \text{x } 0.396 \text{ x } 10^{-24} \text{ cm}^3 \qquad (20)$$

where Eg is the bandgap value resolved through the UV transmission spectrum.

The prominent frequency dielectric constant of materials is a prime specification for enumerating the physical or electronic properties of materials. All the above specifications were evaluated and manifested in **Table-1**. These values are in proficient compatibility with previously delineated values [14]. From these results, it is conspicuous that plasma energy, penn gap and Fermi energy of TU are increased because of the inclusion of SATH. Moreover, the polarizability of TU was also increased by the supplement of SATH.

Table-1: Electronic Specifications of TU and STATH single crystals

Specifications	TU	STATH
Plasma energy (hωp)	17.49 eV	27.07 eV
Penn gap (Ep)	2.80 eV	4.08 eV
Fermi Energy (E_F)	13.39 eV	23.96 eV
Electronic polarizability (manipulating Penn analysis)	1.98×10^{-23} cm^3	2.01×10^{-23} cm^3
Electronic polarizability (manipulating Clausius–Mossotti relation)	1.99×10^{-23} cm^3	2.02×10^{-23} cm^3
Electronic polarizability (manipulating bandgap)	1.77×10^{-23} cm^3	$1.75 \times 10^{-23} cm^3$

3.5 SHG Analysis

The Second harmonic generation efficiency of STATH was investigated by Kurtz and Perry powder technique. A Q- switched mode locked Nd:YAG laser of wavelength 1064 nm with a pulse width of 8 ns and a replication rate of 10 Hz was permitted to pass through the powdered sample (STATH) which was kept in a capillary tube. The excretion of green light with a wavelength of 532 nm affirms the second harmonic generation efficiency of STATH. A second harmonic out signal of 119 mV was procured for an input beam of energy 2.149 mJ /pulse for STATH. For the same incident radiation, the output signal was perceived as 79 mV for KDP. Hence it is established that the SHG efficiency of STATH crystal is 1.506 times that of standard potassium dihydrogen phosphate (KDP).From the results, it is perceptible that STATH has the prohibitive SHG efficiency and hence it is an optimistic NLO crystal for optoelectronic applications.

4. Conclusion

Single crystals of TU and STATH have been auspiciously grown by the slow evaporation technique, from aqueous solution. The X-ray diffraction analysis substantiated the orthorhombic structure of both the samples. From the UV–Vis–NIR spectroscopy, the optical constants were enumerated for both the samples. The particulars about the chemical composition of the grown crystals are procured by employing an analytical technique called Energy-dispersive X-ray spectroscopy. The dielectric test displays that the net polarization value of the grown samples decreases with the increase in frequency and becomes minimum at optical frequency span. From the SHG efficiency test, it is conspicuous that the efficiency of STATH crystal is 1.506 times that of standard potassium dihydrogen phosphate (KDP). As a consequence of its prominent NLO efficiency, STATH is a deserving material for optoelectronics applications.

Acknowledgement

The authors desire to recognize IISC-Bangalore, India, for presuming the prerequisites for SHG measurement. The authors are also grateful to STIC Cochin, India, for presuming Single XRD, Powder XRDand UV instrumental facilities. The authors are also desire to recognize SASTRA University, Thanjavur, India for presuming the prerequisites for EDX. The authors are thankful to St. Joseph's College, Trichy, India, for providing the prerequisites for Dielectric measurement. The authors are also grateful to Prof. Sundara Bharathi for his invaluable support.

References

1. D. Xu, D.R.Yuan,N. Zhang,W.B.Hou,M.G.Liu,S.Y.Sun,M.H.Jiang, J.Phys.D26(1993)B230.
2. I.Ledous,Synth.Met.54(1993)123.
3. H.Q. Sun, D.R. Yuan, X.Q. Wang, X.F. Cheng, C.R. Gong, M. Zhou, H.Y. Xu, X.C. Wei, C.N. Luan, D.Y. Pan, Z.F. Li, X.Z. Shi, Cyrst.Res.Technol. 40 (2005) 882.
4. P.M. Ushasree, R. Muralidharan, R. Jayavel, P. Ramasamy, J.Cryst.Growth 218 (2000)365.
5. J. Ramajothi, S. Dhanuskodi, K. Nagarajan, Cyrst.Res.Technol. 39 (2004) 414.
6. R.BairavaGanesh,V.Kannan,K.Meera,N.P.Rajesh,P.Ramasamy, J.Cryst.Growth282(2005)429.
7. K.Sethuraman,R.RameshBabu,R.GopalakrishnanandP.Ramasamy Cyrstal Growth & Design 8 (2008) 6.
8. B.Neelakantaprasad, G.Rajarajan, D.Marimuthu, J.Senthikumar, C. Sadeeshkumar,B. Ravi, A.Jegatheesan, RASAYAN J.Chem.7 (2014) 3.
9. H.O.Mercy,L.F.Warren,M.S.Webb,C.A.Ebbers,S.P.Velsko,G.C.Kennedy,G.C.Catella,Appl.Opt.31(1992)5051.
10. V.Venkataramanan,S.Maheswaran,J.N.Sherwood, H.L.Bhat,J.Cryst.Growth.179(1997)605.
11. V.Venkataramanan,G.Dhanaraj, V.K.Wadhawan,J.N.Sherwood,H.L.Bhat,J.Cryst.Growth.154(1995)92.
12. V.Kannan,N.P.Rajesh,R.BairavaGanesh,P.Ramasamy,J.Cryst. Growth,269(2004)565.
13. N.P.Rajesh,V.Kannan,M.Ashok,K.Sivaji,P.SanthanaRaghavan,P.Ramasamy,J.Cryst.Growth,262(2004)561.
14. Sagadevan Suresh, Optik 125 (2014) 1223-1226.

*****